

# XMM-Newton EPIC & OM observations of Her X-1 over the 35 day beat period

Silvia Zane<sup>1</sup>, Gavin Ramsay<sup>1</sup>, Mario A. Jimenez-Garate<sup>2</sup>, Jan Willem den Herder<sup>3</sup>, Charles J. Hailey<sup>4</sup>

<sup>1</sup>*Mullard Space Science Laboratory, University College London, Holmbury St. Mary, Dorking, Surrey, RH5 6NT, UK*

<sup>2</sup>*MIT Center for Space Research, 77 Massachusetts Avenue, Cambridge, MA 02139, USA*

<sup>3</sup>*SRON, the National Institute for Space Research, Sorbonnelaan 2, 3584 CA Utrecht, The Netherlands*

<sup>4</sup>*Columbia Astrophysics Laboratory, Columbia University, New York, NY 10027, USA*

Accepted 23 Jan 2004:

## ABSTRACT

We present the results of a series of XMM-Newton EPIC and OM observations of Her X-1, spread over a wide range of the 35 day precession period. We confirm that the spin modulation of the neutron star is weak or absent in the low state - in marked contrast to the main or short-on states. During the states of higher intensity, we observe a substructure in the broad soft X-ray modulation below  $\sim 1$  keV, revealing the presence of separate peaks which reflect the structure seen at higher energies. The strong fluorescence emission line at  $\sim 6.4$  keV is detected in all observations (apart from one taken in the middle of eclipse), with higher line energy, width and normalisation during the main-on state. In addition, we report the detection of a second line near 7 keV in 10 of the 15 observations taken during the low-intensity states of the system. This feature is rather weak and not significantly detected during the main-on state, when the strong continuum emission dominates the X-ray spectrum. Spin resolved spectroscopy just after the rise to the main-on state shows that the variation of the Fe  $K\alpha$  at 6.4 keV is correlated with the soft X-ray emission. This confirms our past finding based on the XMM-Newton observations made further into the main-on state, and indicates the common origin for the thermal component and the Fe  $K\alpha$  line detected at these phases. We also find that the normalisation of the 6.4keV line during the low state is correlated with the binary orbital phase, having a broad maximum centered near  $\phi_{orbit} \sim 0.5$ . We discuss these observations in the context of previous observations, investigate the origin of the soft and hard X-rays and consider the emission site of the 6.4keV and 7keV emission lines.

**Key words:** accretion, accretion disks – X-rays: binaries – individual: Her X-1 – stars: neutron

## 1 INTRODUCTION

Her X-1 is one of the best studied X-ray binaries in the sky; this is borne out by the fact that since 2000 there has been more than 30 papers published in refereed journals with “Her X-1” in the title. We list very briefly the most salient observational characteristics which are relevant to the present study. Her X-1 is a binary system, which consists of a neutron star and an A/F secondary star; it has an orbital period of 1.7 day and the spin period of the neutron star is  $\sim 1.24$  sec. It is one of only a few systems which shows a regular variation in X-rays: the 35 day variation is referred to

as the “beat” period throughout this paper, and the phasing on this period is marked as  $\Phi_{35}$ .

The beat cycle begins with a sharp rise in X-ray intensity, which reach the maximum flux,  $F_{max}$ , in less than  $\sim 0.5$  day and then lasts  $\sim 10$  day (“main-on” state). This is followed by a period of low X-ray emission (“low-state”) and later again by a “short-on” phase, during which the X-ray flux reaches  $\sim 1/20F_{max}$  and  $\sim 1/3F_{max}$ , respectively. A second low-state follows until the onset of the next main-on. The spin modulation of the neutron star is most prominent during the main-on state, becoming much less so (if seen at all) during the low-state and increasing again during the short-on (see e.g. Deeter et al. 1998).

The observed X-ray spectrum changes markedly over the beat cycle. However, it has been recognized that the X-ray spectra taken at different beat phases can be fitted using a constant emission model and adding one or more absorption components which vary in column density over the beat period, reaching a maximum value during the low-state (e.g. Mihara et al. 1991, Leahy 2001). This strengthened the idea that the 35 day cycle is due to the precession of an accretion disk, that periodically obscures the neutron star beam.

A rather broad Fe K $\alpha$  emission line at  $\sim 6.5$  keV has been observed by *Ginga* (see Leahy, 2001 and past references therein); line energy and width have been found to vary over both the beat and the spin period (e.g. Choi et al. 1994). Using *ASCA* data taken during the main-on state, Endo, Nagase & Mihara (2000) were able to resolve the feature into two discrete emission lines, at  $\sim 6.4$  keV and 6.7 keV. However, the second feature has never been detected in other observations. With the advent of imaging X-ray satellites with large effective area over a broad energy band and relatively good spectral resolution at energies near 6 keV, it is now possible to resolve the Fe lines with better signal to noise than what was possible using *ASCA*. Moreover, while *ASCA* had a lower limit of  $\sim 0.5$  keV, the energy response of *XMM-Newton* extends down to  $\sim 0.2$  keV and this allows a more accurate quantification of the absorption column density.

Another manifestation of the 35 day cycle is the evolution of the Her X-1 pulse profile at energies above  $\sim 1$  keV. A few other pulsars show pulse shape changes which are correlated with high-low states of X-ray intensity, but they are typically transients such as GX 1+4 (Dotani et al. 1984) and EXO 2030+375 (Parmar, White & Stella 1989) or flaring sources as LMC X-4 (Levine et al. 1991). Her X-1 is unique in having a repetitive evolutionary pattern in pulse changes tied to a regular high-low intensity cycle, and is therefore a subject of continued interest. Particularly successful in explaining the basic features observed by *Ginga* and *RXTE* is the accretion column model by Scott et al. (2000). This model invokes the successive obscuration of a compact pencil beam from the neutron star, two fan beams with size  $\sim 2R_{ns}$  and a more extended scattered component.

At lower energies (below  $\sim 0.7$  keV), the light curve does not show evidence for a similar variety of emission components. Past detections of pulsations in the soft X-rays of Her X-1 obtained using *EXOSAT* (Ögelmen & Trümper 1988), *ROSAT* (Mavromatakis 1993), and *BepoSax* (Oosterbroek et al. 1997, 2000, 2001) only show a broad and quasi-sinusoidal modulation, which is shifted in phase with respect to the maxima observed at higher energies. The phase shift, as measured during the main-on and short-on state, differs from  $180^\circ$ . Under the assumption that soft X-rays are due to the reprocessing of the pulsar beam by the inner edge of the disk, this is usually interpreted as evidence for a tilt angle in the disk (see e.g. Oosterbroek et al. 1997, 2000). As predicted by precessing disk models (Gerend & Boynton, 1976), the hard/soft shift in phase should vary along the beat cycle. The ideal way to test this would be to track the pulse difference over the entire 35 day period. However, past measurements were restricted to the main-on and short-on states, due to the difficulty of detecting a spin modulation during phases in which the system is highly absorbed. Using *XMM-Newton* data, Ramsay et

al. (2002, hereafter R02) reported the first evidence for a substantial change in the phase difference along the beat cycle. We also found that the values of the phase shift observed by *XMM-Newton* during the main-on and short-on differ from those measured in the past at similar beat phases. However, at the time of that paper only three *XMM-Newton* observations, at three different beat phases, had been performed.

To date, Her X-1 has been observed by *XMM-Newton* on 15 separate occasions giving good coverage over the beat period. The first three observations have been discussed in detail by R02 and Jimenez-Garate et al. (2002). Here we report the analysis of the remaining datasets, focusing on results obtained using the broad energy band EPIC detectors and putting our past findings in a broader context. We also present the simultaneous UV observations made using the Optical Monitor (OM). Observations are described in § 2. UV data and timing analysis are presented in § 3 and § 4 respectively, while the behaviour of the Fe feature(s) over the beat, the spin and the orbital period is reported in § 5. Summary and discussion follow in § 6.

## 2 OBSERVATIONS

### 2.1 Instrumental setup and data reduction

*XMM-Newton* has three broad-band imaging detectors with moderate spectral resolution: two EPIC MOS detectors (Turner et al. 2001) and one EPIC PN detector (Strüder et al. 2001). During the observations of Her X-1, PN and MOS1 were configured in timing mode, while MOS2 was configured in either small window or full frame mode. All three EPIC cameras were used in conjunction with medium filters. The Optical Monitor (Mason et al. 2001) was configured in imaging mode, by using the UVW1 and UVW2 filters (effective wavelength 2910 and 2120 Å respectively).

The details of the observations are summarized in Table 1; as previously mentioned, the results from the first three observations have been already reported in detail by R02 and Jimenez-Garate et al. (2002). The raw event files were first examined and corrected for any time anomalies (see R02), and then reduced using the *XMM-Newton* Science Analysis Software v5.3.3. The events from timing mode data were extracted in a way similar as in R02. For datasets taken in full-frame and small window mode, events were extracted from an aperture of  $\sim 40''$  centered on the source and a background, source-free region; the background subtracted spectra were obtained by scaling appropriately for the size of the two regions. Finally, the event arrival times were corrected to the solar system barycenter and to the center of the binary system, using the ephemeris of Still et al. (2001).

### 2.2 Determining the beat phase

The beat period of Her X-1 is known to vary by up to a few days (Baykal et al. 1993). In order to determine how the epochs of the *XMM-Newton* observations relate to the precession cycle, we extracted the *RXTE* ASM (2-10) keV quick-look light curve from the MIT web site and we determined the 35 day phase by computing the time difference

Observation Date	XMM-Newton Orbit	Exp (ksec)	MOS Mean Ct/s	Orbital Phase	35 d Phase
2001 Jan 26	207	10	97.5	0.20–0.26	0.17
2001 Mar 04	226	11	3.6	0.47–0.56	0.26
2001 Mar 17	232	11	11.3	0.52–0.60	0.60
2002 Feb 25	405	10.3	2.5	0.55–0.62	0.46
2002 Feb 27	406	11.7	3.2	0.71–0.79	0.51
2002 Mar 07	410	8.8	5.2	0.40–0.46	0.74
2002 Mar 09	411	7.3	3.4	0.57–0.62	0.79
2002 Mar 15	414	7.3	2.2	0.09–0.14	0.96
2002 Mar 17	415	7.3	130	0.26–0.31	0.02
2002 Mar 27	420	4.4	3.4	0.17–0.20	0.31
2002 Sep 20	509	5.9	2.9	0.56–0.60	0.35
2002 Sep 22	510	7.3	1.8	0.72–0.77	0.41
2002 Oct 04	516	10.3	2.1	0.78–0.85	0.77
2003 Mar 26	603	15.6	2.0	0.81–0.88	0.72
2003 Mar 28	604	6.1	0.5	0.98–0.03	0.75

**Table 1.** Summary of the XMM-Newton observations of Her X-1. For the orbital phasing we use the ephemeris of Still et al. (2001); for the 35 d phasing we define phase 0.0 at the main high state turn-on (see text for a discussion). The count rate refers to the rate in either the MOS1 or MOS2 detector depending on the source intensity. Analysis of the first three datasets has been presented in details in R02 and Jimenez-Garate et al. (2002).

between each observation and the start of the previous rise to maximum. We then took the period to be the time till the next rise to maximum. We estimate the uncertainty on the phase of the beat period to be  $\sim 0.01$ – $0.02$  cycles. The resulting beat phase is reported in Table 1, along with the dates of the observations and the mean X-ray brightness. Note that the last observation has been taken during an eclipse of the primary by the secondary star: this corresponds to the point with the lowest X-ray count rate in Figure 1.

The phase coverage of the XMM-Newton observations over the 35 day period is shown in Figure 1. For comparison, we also show the ASM light curve recorded during a typical cycle. We note that, since the actual period of the X-ray modulation varies around its nominal value of 35 d, the determination of the state of the system (either low, main on or short on) based on a direct comparison with the ASM lightcurve in the top panel must be taken only as indicative.

As we can see, the beat cycle is reasonably well sampled, with most of the exposures taken outside the main-on and short-on phases. Three observations have been performed during states of high intensity: in addition to the main-on and short-on datasets discussed by R02 ( $\Phi_{35} = 0.17$  and  $0.60$ ) we have a further exposure at  $\Phi_{35} = 0.02$ . We note that the ASM lightcurve

### 3 THE UV DATA

The UV emission probably originates from a blend of at least two different components: the illuminated face of the secondary star and the accretion disk. Their relative contribution varies during the orbital motion, and in general is difficult to disentangle. Unlike the X-rays, the UV emission does not show an obvious correlation with the beat period. This is in agreement with the fact that the disk contribution

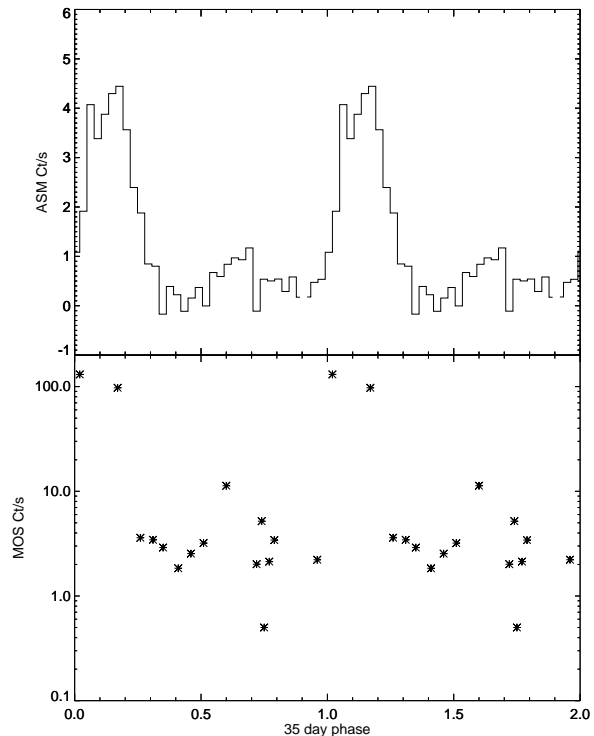


**Figure 1.** Top Panel: a typical RXTE/ASM (2–10) keV light curve of Her X-1 over the 35 day beat period. Bottom Panel: the mean count rate of Her X-1 registered by the EPIC MOS detectors. The lowest count rate corresponds to an eclipse of the neutron star by the secondary.

is on average small (less than 10% as estimated by Boroson et al. 2001). However, it is modulated over the binary orbital period. The UV count rate detected using the two OM filters is shown in Figure 2, as a function of the orbital phase. Note that observations were not always performed in both filters, and in the last two exposures no UV measurements were made. The illuminated secondary star is expected to dominate around  $\phi_{binary} \sim 0.5$ . As we can see, near this orbital phase the UV flux measured by OM reaches a broad maximum, similar to that found using IUE in the 1750–1850Å band (e.g. Vrtilik & Cheng 1996). However, there is a flux decrease at  $\phi_{binary} \sim 0.5$ , possibly due to the fact that part of the secondary star is shadowed by the accretion disk or to a warp in the disk itself.

The rise from the eclipse ( $\phi_{binary} \sim 0.1$ – $0.3$ ) is steeper in UVW1 (longer wavelength) than in UVW2. Since, at these orbital phases, the accretion disk mainly contributes to the UV flux, this is consistent with a scenario in which, after the eclipse, the regions of the disk farthest from the neutron star come into view first.

### 4 TIMING ANALYSIS

#### 4.1 Search for modulation close to the spin period

The spin period of Her X-1 has been found to vary from  $\sim 1.23772$  s to  $1.23782$  s, with alternating phases of spin-up and spin-down (Parmar et al. 1999, Oosterbroek et al. 2001). Furthermore, it can vary significantly on relatively short time scales. The values of the spin period measured using

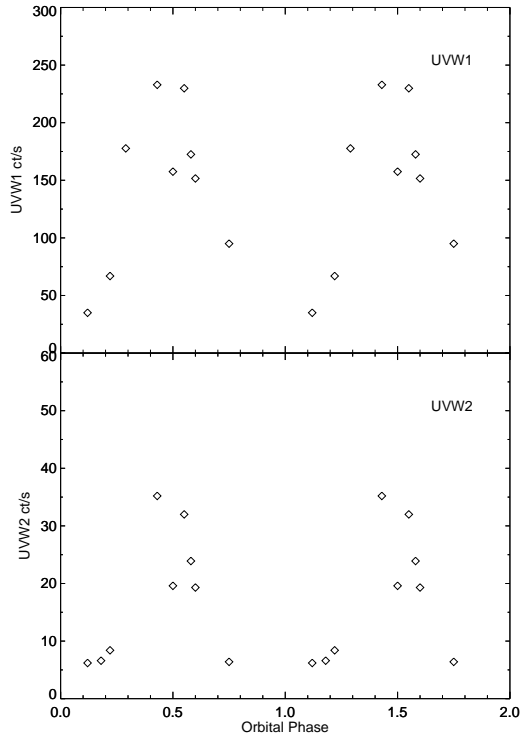


**Figure 2.** Top Panel: The UVW1 (top panel) and UVW2 (bottom panel) data folded on the orbital period. data have been phased by using the ephemeris of Still et al. (2001).

the first three *XMM-Newton* observations were reported by R02: using the PN detector, we found 1.237774 s, 1.237753 s and 1.237751 s, respectively. The first measure confirmed the slow-down trend monitored by *BeppoSax* (Oosterbroek et al. 2000) and *Chandra* (Burwitz, private communication); although we observed a slight decrease in the two following epochs.

We performed a search for pulsations using a Discrete Fourier Transform for all the new datasets, finding a strong evidence of pulsations only in one case (revolution 415). This is the only new exposure taken outside the low state, precisely during the main-on at  $\Phi_{35} = 0.02$ . The corresponding spin period, as obtained from the EPIC PN data, is 1.237777(1) s, where the number in parenthesis represents the error on the last digit as determined by using the Cash (1979) statistic. The spin period is just slightly increased with respect to the value measured by *XMM-Newton* in 2001.

All the remaining datasets showed amplitude spectra with only weak or no significant peaks close to the expected spin period. In order to investigate further the possible presence of a modulation, we folded all the datasets on the most recent measured period, i.e. 1.237777 s, by using 25 phase bins. We then fitted a constant value to the resulting light curve and determined the  $\chi^2$ . Therefore, we expect a poorer fit in datasets with a stronger spin modulation. Since the profile of the folded light curve varies considerably in the soft and hard energy band, we split the events into two energy ranges: 0.3-0.7 keV and 2-10 keV. The resulting  $\chi^2$  is shown in Figure 3, as a function of the 35 day phase. For 1 degree of freedom (the value of the period), the difference to the fit is  $\Delta\chi^2=2.71$  at the 90 percent confidence level.

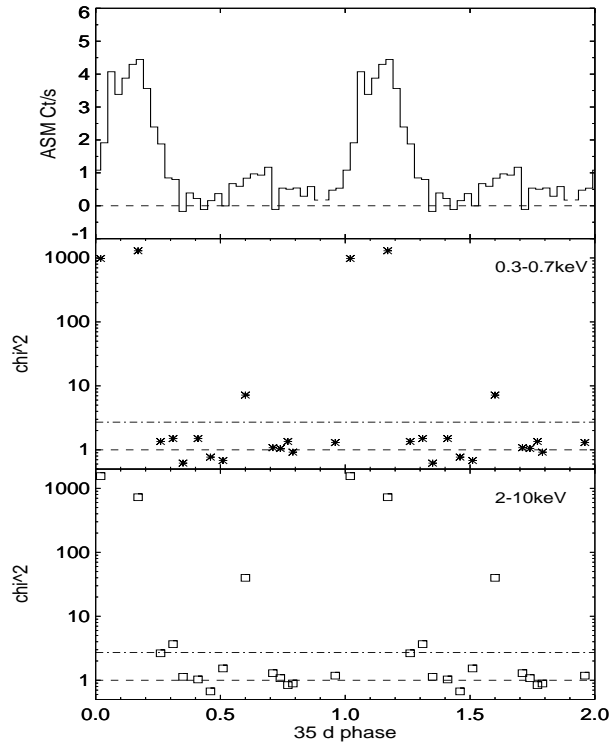


**Figure 3.** Top panel: the mean ASM X-ray light curve over the 35 day cycle. Middle panel: the  $\chi^2$  obtained by fitting a constant value to the 0.3-0.7 keV folded light curve. Bottom panel: same but for 2-10 keV folded light curve. In folding the data we folded the data on the spin period determined using a Discrete Fourier Transform (main-on or short-on observations) or, when unavailable, the more recent measure of 1.237777 s. The  $\chi^2$  is computed by using 25 phase bins.

Using this method we find that, outside the main-on and short-on states there is evidence for significant modulation above 2 keV in the two datasets taken at  $\Phi_{35}=0.26$  and 0.31. In the first case (which is one of those already reported by R02) the  $\chi^2$  increases above the 90 percent confidence level if we reduce the number of phase bins from 25 to 20.

Defining the amplitude as (max-min/mean) of a fitted sinusoid, we find an amplitude of 11 and 13 percent for  $\Phi_{35}=0.26$  and 0.31, respectively. Previous observations of Her X-1 during the low state include Coburn et al. (2000), who found a spin modulation of  $\sim 13$  percent (assuming the same definition as ours) in the 3–18 keV range using *RXTE* data in an anomalous low state, while Mihara et al. (1991) determined an upper limit for the pulsed fraction of 2.4 percent in the 1.2-37 keV energy range using *Ginga* data.

## 4.2 Spin-resolved light curves

In Figure 4, we show the spin profiles of Her X-1 as derived for those observations in which we detected a significant modulation in the 0.3-0.7 keV or in the 2-10 keV energy band. Due to the uncertainty in the spin period at each epoch, the spin phases are not on the same absolute scale. Therefore, only the relative phasing between the light curves in different energy bands *taken during the same observation* is physically meaningful (see § 4.3).

The change of the spin profile of Her X-1 in different energy bands has been well documented in the literature. In

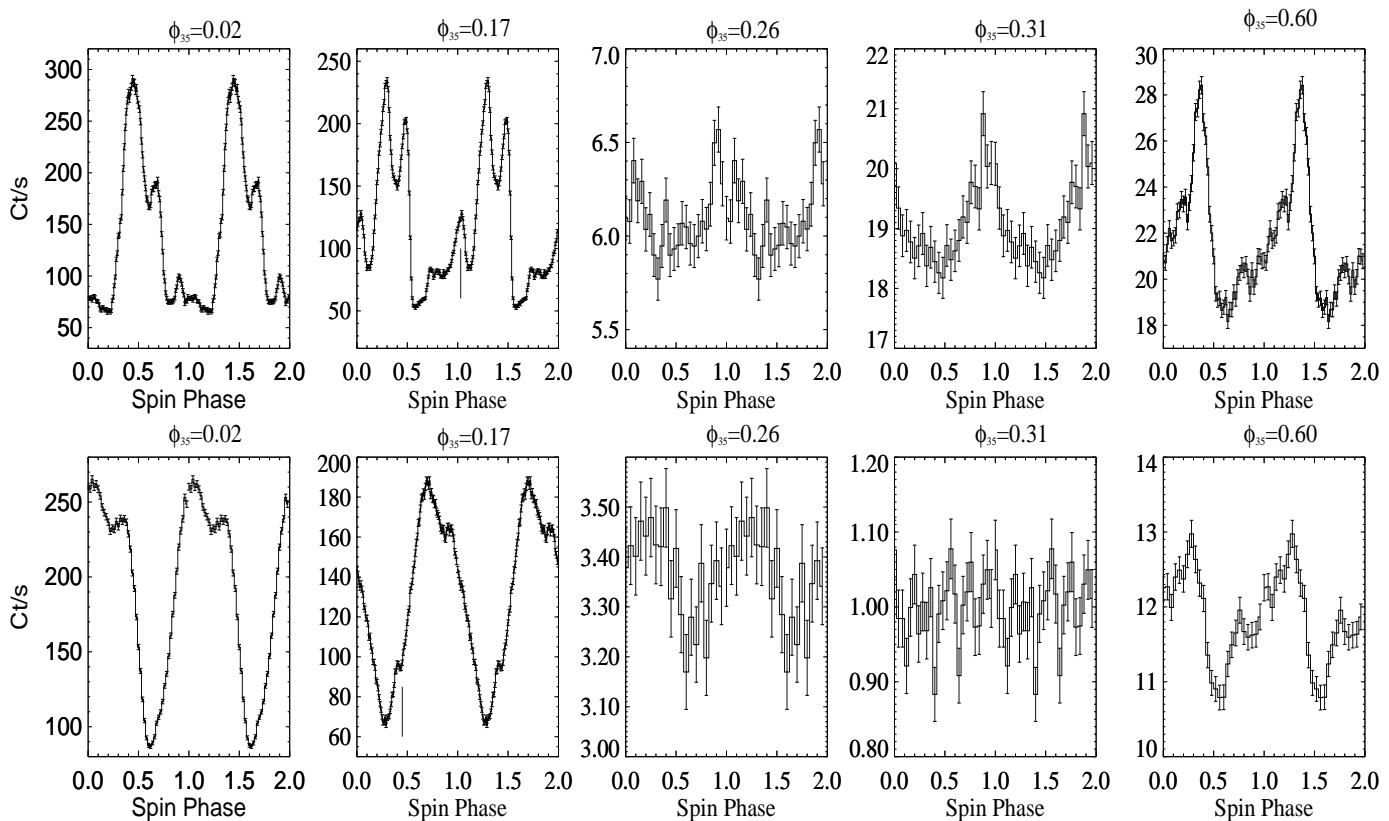


**Figure 4.** Upper panel: the EPIC PN spin profile in the 2-10 keV band as a function of the 35 day cycle. Lower panel: as above but for the 0.3-0.7 keV band. In all panels, because of the uncertainty in the spin period in each epoch, the spin phases are not on an absolute scale. The two vertical lines at  $\Phi_{35} = 0.17$  mark the second atypical peak in the interpulse (hard band) and the small “notch” like feature (soft band) discussed in the text.

order to compare the spin profiles obtained by using *XMM-Newton* with the previously published data, we take as reference, in the range above  $\sim 2$  keV, the work of Deeter et al. (1998) and Scott et al. (2000). These authors reported the variation of the hard X-rays light curve obtained by *Ginga* and *RXTE* over a wide range of beat phases.

As we can see, the *XMM-Newton* light curves obtained shortly after the main-on turn on ( $\Phi_{35}=0.02$ ) in the 2-10 keV energy band closely resemble most of the main-on states previously reported. The only exception is that the small peak observed during the inter-pulse (at  $\phi_{spin}=0.9$  in Figure 4) appears slightly more sharp than previously reported. At the next main-on beat period,  $\Phi_{35}=0.17$ , we detect an atypical profile, with a second large peak in the interpulse on the leading side of the main pulse (the feature occurs at  $\phi_{spin}=0.05$  in Figure 4). The peak becomes more prominent as the high state progresses, and has been observed only occasionally in Her X-1: it is present in the *Ginga* data taken during the main-on state “D” by Deeter et al. (1998), at the two beat phases  $\Phi_{35}=0.073$  and 0.162. However, it was not present in the other of their main-on observations nor in those discussed by Scott et al. (2000). Deeter et al. (1998) noted that such atypical profile is similar to a previous one recorded by using *Kvant* (Sunyaev et al. 1988) and suggest it may be due to a reduction in the accretion rate.

Moving later in beat phase, the detected amplitude of the hard X-ray modulation decreases sharply at  $\Phi_{35}=0.26$  and  $\Phi_{35}=0.31$ : here the modulation is broad and quasi-

sinusoidal. There is evidence of a double peaked structure at  $\Phi_{35}=0.26$ : R02 show the hard X-ray modulation resolved into finer energy bands and find that at this beat phase modulation at the hardest energies is broad and single-peaked. Note that the profile obtained at  $\Phi_{35}=0.31$  is less certain, since it has been obtained by folding data over the most recent measured period and not using the period measured at the time of the observation. However, we have explored the effect of folding the data on slightly different spin periods, centered around 1.237777 s: the resulting folded light curves are very similar. The profile detected during the short-on ( $\Phi_{35}=0.60$ ) is similar to previous observations at a similar beat phase, although the high signal to noise ratio of the *XMM-Newton* data revealed a more complex structure during the rise of the main peak.

The high throughput of *XMM-Newton* allows us to obtain a light curve with very high signal to noise ratio also in the soft X-rays (0.3–1 keV). Consistent with past measurements, the spin profiles of the soft X-ray band in Figure 4 show a basically sinusoidal shape. However, in both main-on observations the broad peak is cut by a dip which has not been seen before. Further, data taken at  $\Phi_{35}=0.17$ , show a small “notch” like feature preceding the maximum (at  $\phi_{spin}=0.4$  in Figure 4). During the short-on ( $\Phi_{35}=0.60$ ) the modulation is broader, with evidence for a fairly complex substructure during the leading edge of the peak.

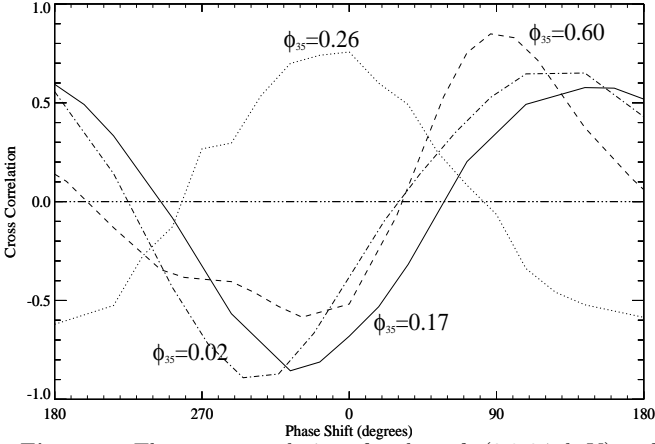


**Figure 5.** The cross correlations for the soft (0.3-0.7 keV) and hard (2-10 keV) light curves at four different 35 day phases.

### 4.3 The phase shift between the soft and hard light curves

R02 found that the phase shift between the soft and hard X-ray light curves, folded on the spin period, varied over the beat period. To determine how the dataset taken at  $\Phi_{35}=0.02$  compared with these previous observations we cross-correlated the hard and soft light curves (see R02 for details). This is the only new observation that can be used for such purpose, since the others do not show a significant modulation in both soft and hard X-rays. As we can see, the two observations taken during the main-on have a very similar correlation, with data taken at  $\Phi_{35}=0.02$  showing a strong anti-correlation and a phase shift between the maxima of the soft and hard light curves of  $\sim 130^\circ$ . This difference in phase is slightly smaller than what was observed at  $\Phi_{35}=0.17$ , and consistent with the general trend over the beat period.

## 5 SPECTRAL ANALYSIS: THE VARIATION OF FE COMPLEX

### 5.1 Line variation over the beat cycle

The integrated X-ray spectra of Her X-1 over the 35 day cycle have been modeled by many authors (e.g. Mihara et al. 1991, Oosterbroek et al. 1997, Coburn et al. 2000, Oosterbroek et al. 2000, Choi et al. 1994, Leahy 2001). In accordance with these studies, the main on, short on and low states all require a two component continuum with a basic emission spectrum and an absorbed component whose strength is maximum during the low states. The natural interpretation is that the 35 day variation is due to the occultation of the neutron star beam by the intervening accretion disk. Model fitting of the *XMM-Newton* spectra obtained using the first three datasets has been reported by R02 and confirm this picture. Here, we used the same model for fitting the newest datasets: since the overall fits do not show new characteristics we do not discuss further the details of the overall spectral shape.

Instead, we focus on the behaviour of the X-ray spectra near the Fe line component(s), detected in the past around  $\sim 6.6$  keV. As shown by R02, the central energy of the flu-

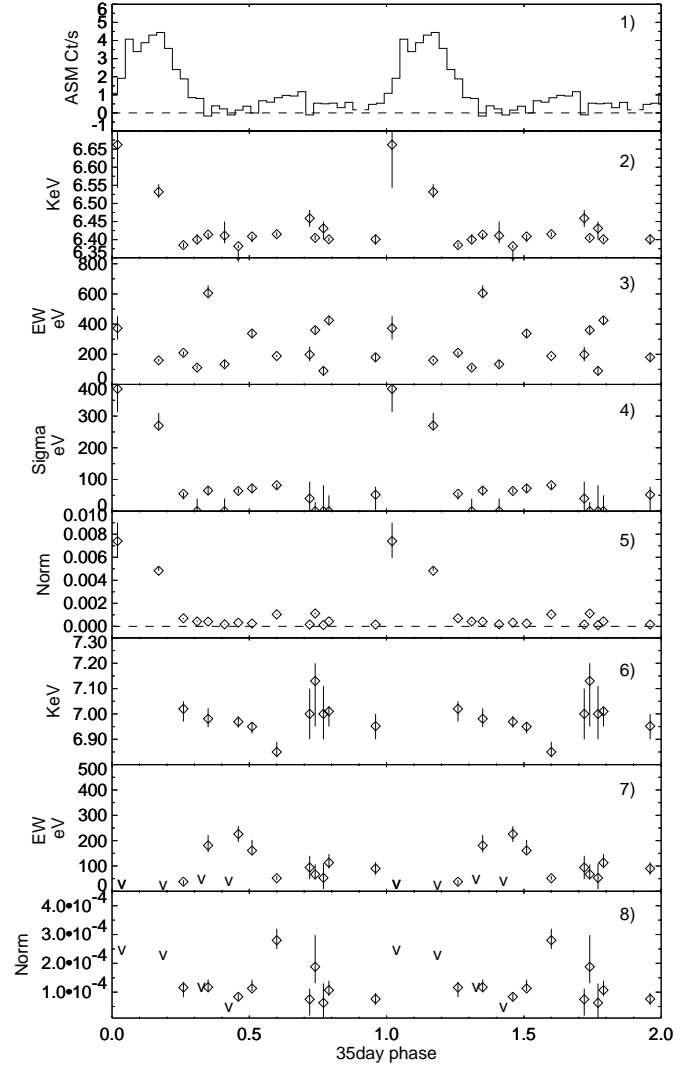


**Figure 6.** Variation of the  $K\alpha$  and Fe XXVI line parameters along the beat cycle, as measured with EPIC PN. From the top: 1) mean ASM light curve; 2)-5) central energy, equivalent width (EW), width and normalization of the prominent  $K\alpha$  Fe emission line; 6)-8) central energy, EW and normalization of the Fe line at  $\sim 7$  keV. For those datasets where the second feature is undetected, we report upper limits to the EW and normalization, at the 90 percent confidence level (“v” symbols).

orescent line varies over the beat period, increasing during the main on. However, only three epochs were reported in that paper.

In order to fit the spectra, we restricted the energy range to 4-10 keV and fitted an absorbed power law with one or more Gaussians. The power law and Gaussian parameters were then fixed and the energy range 0.3-4 keV included. The absorption component was allowed to vary and we included a blackbody component and a neutral partial covering model if required. This allows us to fix the absorption components at an appropriate level, which is crucial since, for large values of the column density, a characteristic absorption feature appears at  $\sim 7.1$  keV. This feature may affect the identification of the emission Fe lines, therefore it has to be modeled carefully.

Consistent with R02, we found that a prominent fluorescent line is detected at all beat phases (apart from obser-

vation taken during at mid-eclipse), with a central energy that varies between  $\sim 6.4$ - $6.6$  keV and is highest during the main-on. However, the most striking result is the detection of a second component, an Fe XXVI line at  $\sim 7$  keV, which is only present outside the main-on. This line was not reported by R02, but a closer analysis of the two observations taken at  $\Phi_{35} = 0.26$  and  $0.60$  revealed its detection in both datasets. The line parameters are reported, as a function of the beat phase, in Figure 6.

We find that the equivalent width (EW) of the  $K\alpha$  Fe line shows a variation through the beat cycle, with no trend being visible. This is likely to be due to a varying continuum, since the  $K\alpha$  Fe line normalisation is highest during the main-on state while it remains low and almost constant at other 35 day phases. Similarly, the line width is greatest during the main-on state. The energy of the second component remains approximately constant at  $\sim 7.0$  keV, except during the short-on state where it is significantly lower ( $\sim 6.85$  keV). The feature is strongest (larger EW) during the states of low X-ray intensity, although it is undetectable in some of the exposures in this phase range. On the other hand, its normalisation is strongest during the short-on. In some of the observations, we do not find evidence for a significant Fe XXVI line. In order to determine upper limits to EW and line normalisation, we added a Gaussian component to the best fit spectral model, by fixing the central energy at 7 keV and the width at 0.1 keV. The upper limits obtained for the datasets taken during the main-on are consistent with the line being undetected because of the strong continuum emission.

In order to show the significance of both the Fe features, we show in Figure 7 the X-ray spectrum between 5-9 keV for  $\Phi_{35}=0.02$  and  $\Phi_{35}=0.79$ . The solid line is the best fit spectral model with the normalisations of the two Gaussian components set to zero. We find no evidence for the presence of a Compton downscattered shoulder (expected near  $E_0 - E_0/(m_e c^2 + E_0)$  where  $E_0$  is the centroid of the line) of the kind recently observed in HETGS *Chandra* spectra of the high mass X-ray binary GX 301-2 (Watanabe et al. 2003).

## 5.2 Pulse-resolved spectroscopy

The variation of the Fe  $K\alpha$  line over the neutron star spin period and its correlation with the thermal or non-thermal spectral components was studied by R02. We found no evidence for a significant variation in the line parameters at  $\Phi_{35}=0.26$  or  $0.60$ . In contrast, the observation made during the main-on ( $\Phi_{35}=0.17$ ) showed a clear correlation between the EW of the 6.4keV line and the soft X-ray light curve. This supported the idea of a common origin for the  $\sim 6.4$  keV fluorescent line and the thermal flux.

The new data taken during the main-on ( $\Phi_{35}=0.02$ ) can be used to test this scenario further. We phased all the events on the spin period determined in §4 and extracted spin-phase resolved spectra. Details of the model fitting are as in §5.1. Results are reported in Figure 8, together with the soft and hard X-ray light curves.

The shape of the EW variation is broadly similar to the profile at  $\Phi_{35}=0.17$  (R02), although that observation shows a more ‘top-hat’ profile. Consistent with R02, we find in the main-on state that both the line normalization and the EW

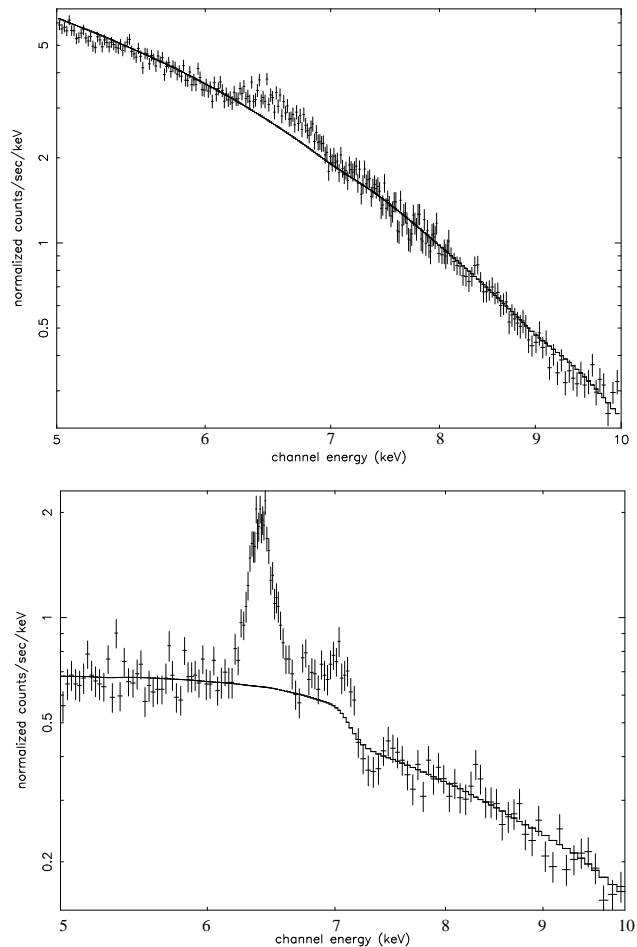


**Figure 7.** The spectral region around 6.6keV from  $\Phi_{35}=0.02$  (top) and  $\Phi_{35}=0.79$  (bottom). The y-axis is the normalised counts, i.e. the number of counts per energy bin per second, as measured by EPIC PN. In both panel a solid line shows the best fit after the normalisation of the one or two Gaussian components have been set to zero.

follow the soft X-ray light curve and are anti-correlated with the hard, non-thermal flux emitted above 2 keV.

## 5.3 Variation of Fe complex over the orbital period

Further information about the origin of the Fe  $K\alpha$  6.4keV line can be obtained by observing its variation over the orbital period. This is shown in Figure 9, for all observations taken outside the main-on. The average line normalization is  $2 - 4 \times 10^{-4}$  counts/cm<sup>2</sup>/s, with larger peaks at  $\sim 10^{-3}$  counts/cm<sup>2</sup>/s and a dip at  $\phi_{binary} = 0.43 - 0.56$ . (The line normalisation during the main-on state is greater by a factor if  $>5$ - $10$  compared to the low state). The line is not detected during the middle of the eclipse, at which point the upper limit on the line normalisation is  $3.7 \times 10^{-5}$  counts/cm<sup>2</sup>/s.

In the previous section we showed that during the main-on state the line normalisation phased on the spin period is correlated with the soft X-ray light curve suggesting a common origin for the thermal soft X-ray emission and the 6.4keV line. We now find that in the low state the line nor-

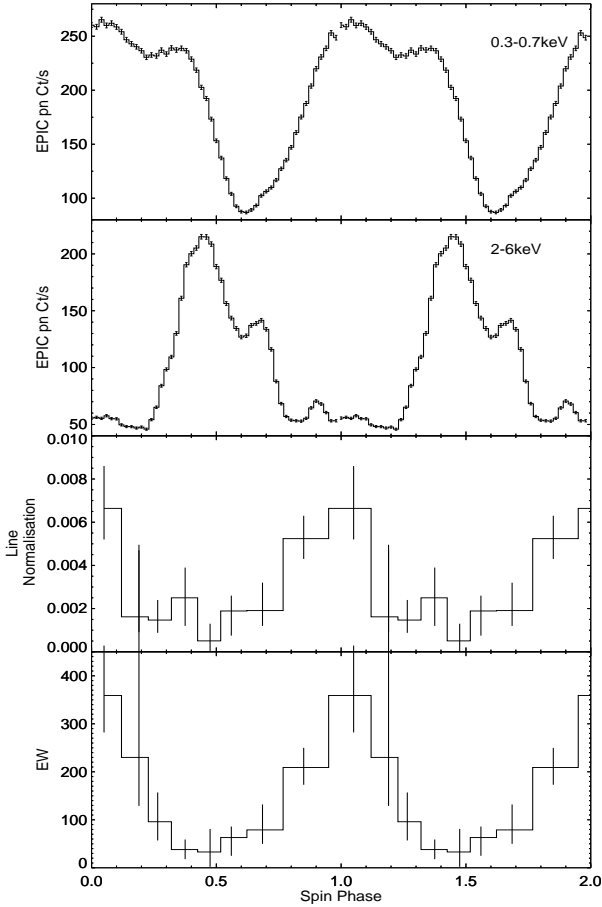


**Figure 8.** The observation made using the EPIC PN detector at  $\Phi_{35}=0.02$ . From the top panel: the light curve in the 0.3-0.7 keV band; the 2-6 keV band; the Fe  $K\alpha$  line normalisation and EW as a function of the spin phase.

malisation is correlated with the orbital period. We go onto explore this further in §6.3.

## 6 DISCUSSION

We have reported the results based on EPIC and OM data for a set of *XMM-Newton* observations of Her X-1. Consistent with past reports, we find that the spin modulation of the neutron star is most prominent during the main-on and short-on state, becoming not significant during the low state. These data sets allow us to follow the change in the relative phasing of thermal and non-thermal emission and the change in the pulse profile over the beat period. The large collective area of *XMM-Newton* and its good response down to soft X-rays also revealed a complex substructure in the light curve in the softest and less well studied energy band.

Data taken during the main on, at  $\Phi_{35} = 0.02$ , show a common phase modulation between the fluorescent Fe  $K\alpha$  line and the soft emission, confirming the results found by R02 at  $\Phi_{35} = 0.17$ . Moreover, for the very first time in CCD non grating spectra, we report evidence for a second Fe line, with central energy near  $\sim 7$  keV, which is only visible out-

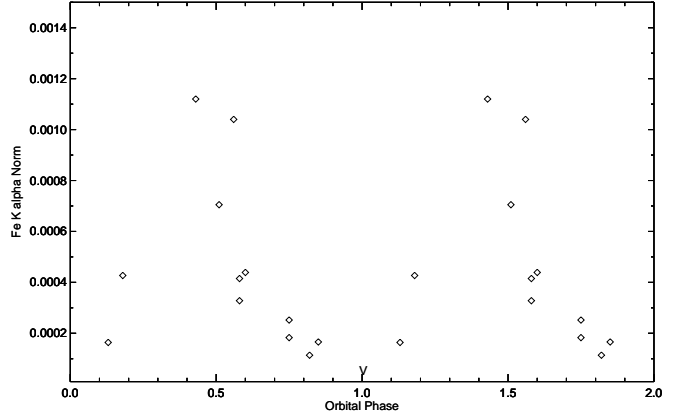


**Figure 9.** The Fe 6.4keV  $K\alpha$  line normalisation as a function of the orbital phase, for all observations taken outside the main-on. Data have been taken with EPIC PN. Only an upper limit has been obtained from the observation taken during the eclipse (arrow).

side the main-on state. We now proceed by discussing some physical interpretations for our results.

### 6.1 The spin-resolved light curves: evidence for structure in soft X-rays (0.3 – 1 keV)

The complex, multi-peaked structure of the pulse profile of Her X-1 above  $\sim 1$  keV and its evolution pattern over the beat cycle is the subject of several studies. The basic features of the pulse profile are nominally explained by the oblique rotator model (Lamb, Pethick & Pines 1973), but there are still many unresolved questions regarding the details of the mechanism, such as whether the radiation pattern is best described by a superposition of ‘fan’ and ‘pencil’ beams and whether the obscuring material that modifies the visibility of the direct beams from the neutron star contributes to the pulse formation. Particularly successful in explaining the pattern observed by *RXTE* and *Ginga* is the accretion column model by Scott et al. (2000). This model invokes the successive obscuration of a direct beam (that originates from the polar caps of the neutron star), two fan beams focussed in the antipodal direction (possibly due to cyclotron backscattering) and a more extended scattered halo. As the main-on progresses, the inner edge of the accretion disk cover first one of the fan beam components, then the direct pencil beam and then the second fan beam component.

In contrast, the pulsation detected below  $\sim 1$  keV using *EXOSAT* (Ögelmen & Trümper 1988), *ROSAT* (Mavroumatakis 1993), and *BeppoSax* (Oosterbroek et al. 1997, 2000, 2001) is broad and quasi-sinusoidal. This emission is thermal and probably originates in the inner edge of the disk, that partially intercepts and reprocesses the hard X-rays from the neutron star. *XMM-Newton* data taken during the main-on have an excellent signal to noise ratio and allow us to resolve a substructure in the soft X-ray light curve. The 0.3-0.7 keV pulse profile observed at  $\Phi_{35}=0.02$  clearly shows the presence of two separate pulses, at  $\phi_{spin} \sim 0.0 - 0.1$  and  $\phi_{spin} \sim 0.3 - 0.4$  in Figure 4 (the value of the absolute spin phase is arbitrary). Similar features are also evident in data taken later in the beat cycle: at  $\Phi_{35}=0.17$  the pulse



profile shows two maxima (at  $\phi_{spin} \sim 0.7$  and  $\phi_{spin} \sim 0.9$  in Figure 4) and a small “notch” like feature preceding the main pulse (at  $\phi_{spin}=0.4$  in Figure 4). During the short on ( $\Phi_{35}=0.60$ ), the soft X-ray modulation is broader, more sinusoidal, and exhibits a complex substructure in the leading edge of the pulse followed by a faster decay.

Whether these features reflect an intrinsic complexity in the thermal and geometrical properties of the reprocessing region or keep memory of the structure of the illuminating beam(s) is unclear. However, it is worth noticing that during all three beat phases with bright emission, the features detected in the soft light curves qualitatively resemble those of the corresponding hard band. The two maxima observed in the softer band during the main-on ( $\Phi_{35}=0.02, 0.17$ ) have a phase separation similar to that of the two main peaks observed in the 2-10 keV range, i.e.  $\Delta\phi_{spin} \sim 0.2 - 0.3$ . Similarly, the small “notch” preceding the main pulse at  $\Phi_{35}=0.17$  may be associated with the atypical pulse observed at higher energies (both precede the main peak by  $\Delta\phi_{spin} \sim 0.25 - 0.3$ ). If these associations are correct, i.e. if at least some of the main characteristics of the neutron star beam are not “washed out” during the reprocessing of hard X-rays, this means that the radiative time scale in the inner edge of the disk is much smaller than the photon travel time. Moreover, the reprocessing region cannot be too extended in size. This may be explained by a high inclination angle of the disk and/or a highly warped inner edge, in which case only a fraction of the inner region of the disk intercepts the neutron star beam. Alternatively, the reprocessing of the neutron star beam may be dominated by a shocked, optically thick hot spot instead of being distributed over the entire inner edge. A similar situation is observed in SW Sex stars (see e.g. Dhillon et al. 1997, Groot et al. 2000 and their Figure 6), where the hot spot region is formed through a shock that occurs along the stream trajectory, but well inside the accretion disk.

## 6.2 The pulse period and the change in the phase shift between soft and hard emission

Given the complexity of the source, pulse-phase spectroscopy is of paramount importance in disentangling the different spectral components observed in Her X-1. Past observations using *Einstein* (McGray et al. 1982) and *Bep-poSax* (Oosterbroek et al. 1997, 2000) showed that, during the main-on state, the maximum of the thermal component and the power-law components are shifted by  $\sim 250^\circ$ . The departure from a phase shift of  $180^\circ$  is usually associated with a disk having a tilt angle, under the assumption that the soft X-rays originate in the layers of the disk that intercept and reprocess the neutron star beam. The first evidence for a change in the pulse difference, as measured at three different  $\Phi_{35}$  using *XMM-Newton*, has been reported by R02. R02 found that during the main-on state ( $\Phi_{35}=0.17$ ) the soft and the hard X-ray pulse profiles were strongly anti-correlated and that the phase shift between the soft and hard maxima was  $\sim 150^\circ$ . This was in contrast to previous observations made during the main-on. Moreover, the phase shift between these components was significantly different in the *XMM-Newton* observations performed at  $\Phi_{35}=0.26$  and  $0.60$ . This led to the suggestion that, during the first three exposures, the tilt angle of the accretion disk was chang-

ing substantially (R02). In contrast with past observations (Oosterbroek et al. 2000), R02 did not detect a symmetric state at  $\Phi_{35} \sim 0, 0.5$ . If the reprocessing region is located at or near the inner region of the disk, such lack of symmetry may indicate that the disk is strongly warped (Heemskerck & van Paradijs 1989). In order to further monitor the phase shift over the beat cycle, we presented a new measure of the pulse difference, taken during the main-on ( $\Phi_{35} = 0.02$ ). We find that the trend detected by R02 is confirmed, and the change in the tilt angle appears to be smooth and continuous over the beat cycle.

Possible recent changes in the structure of the inner layers of the disk have been also discussed by Oosterbroek et al. (2001), who detected a rapid spin down in Her X-1 following an anomalous low state. This spin down was not accompanied by a significant simultaneous change in the mass accretion rate (Oosterbroek et al. 2001). Instead, it was more plausibly associated with changes in the structure of the outer magnetosphere of the neutron star and/or in the inner disk layers. These observations impose important constraints on any theory modeling the accretion torques and phenomena related to the inner edge of the disk in Her X-1.

## 6.3 The Fe K $\alpha$ line

The strong emission line at  $\sim 6.4$  keV is detected in all *XMM-Newton* observations, with larger broadening and normalization during the main-on. Past reports of Fe features in the spectra of Her X-1 include an ASCA exposure (Endo et al. 2000) and a set of 63 *Ginga* observations analyzed by Leahy et al. (2001). The good coverage of the beat period allowed Leahy et al. (2001) to undertake a systematic study of the line variation along the precession cycle. They found a broad feature near  $\sim 6.5$  keV, with the EW varying considerably between main on, short on and low state. The mean values for each state are 0.48 keV, 0.66 keV, and  $\sim 1.37$  keV, respectively. Similar correlations are not evident in the *XMM-Newton* data, where instead an additional Fe XXVI line, possibly a coronal signature, is detected during the low states (see § 6.4).

Nevertheless, we find evidence for a significant variation of the line energy over the 35 day period: the Fe line emission originates in near neutral Fe (Fe XIV or colder) in the low and short-on state observations, whereas in the main-on the observed Fe K $\alpha$  centroid energies ( $6.65 \pm 0.1$  keV and  $6.50 \pm 0.02$  keV as measured using PN at  $\Phi_{35} = 0.02$  and  $0.17$ ) correspond to Fe XX-Fe XXI (Palmeri et al. 2003). The line centroids observed using the EPIC PN deviate by  $4\sigma$  from the 6.40 keV neutral value. This has been already noticed by R02, who suggested three possible explanations for both the line broadening and the centroid displacement:

- (i) an array of Fe K $\alpha$  fluorescence lines exists for a variety of charge states of Fe (anything from Fe I-Fe XIII to Fe XXIII);
- (ii) Comptonization from a hot corona with a significant optical depth for a narrower range of charge states centered around Fe XX. Similar line broadening has been observed in some low mass X-ray binaries with ASCA (Asai et al. 2000), and Her X-1 spectra exhibit one of the larger equivalent widths within the class;
- (iii) Keplerian motion: if this is responsible for the line

broadening, the Keplerian velocity measured at  $\Phi_{35} = 0.02$  and 0.17 is  $\sim 15500$  and  $\sim 13000$  km/sec, respectively. This gives a radial distance of  $\sim 2-3 \times 10^8$  cm (for a neutron star of 1.4 solar masses), which is close to the magnetospheric radius for a magnetic field of  $\sim 10^{12}$  G.

In addition to these possibilities, we also notice that the region responsible for the Fe  $K\alpha$  line emission is likely to be different for lines observed at different beat phases. The Fe lines have different energies, flux, and broadening in the main-on compared to the low state. While data taken during the main on clearly suggest a correlation between the fluorescent Fe  $K\alpha$  line and the soft X-ray emission, the same is not explicitly evident in data taken during the low state. At such phases, instead, the line is a factor  $> 5$  weaker and is clearly modulated with the orbital period.

The correlation between the UV and the neutral Fe K point to a common origin with the fast rise UVW1 emission. Still, it is hard to distinguish the contributions from the companion and the disk to the Fe K line emission. A large contribution from the companion would explain why the Fe K line is so strong in the low state of Her X-1 compared to other accretion disk sources: in Her X-1 the companion is much larger ( $2.3 M_{\odot}$ ) than for other LMXBs. However, due to the fast rise of the Fe K flux with the orbital phase, the disk origin scenario is still strong.

A possible contribution to the Fe  $K\alpha$  emission may arise from relatively cold material in an accretion disk wind, such as commonly observed in cataclysmic variables (see e.g. Drew 1997). Although no consensus has been reached in the case of low-mass X-ray binaries, in the case of Her X-1 evidence of outflowing gas, possibly a wind or material ablated from HZ Her, has been reported by Anderson et al. (1996) and Boroson et al. (2001). UV lines observed with the FOS and STIS spectrographs on the *Hubble Space Telescope* persist even in the middle of the eclipse, when the X-ray heated atmosphere of the normal star and the accretion disk should be entirely hidden from view. The velocities inferred from the broadening of the N V lines are not constant over a time scale of  $\sim 1$  yr, while a comparison between observations taken at  $\phi_{binary} = 0.10, 0.21$  and  $0.29$  show they are stable over the orbital phase. Between these phases, the velocity of the neutron star is expected to change by  $\approx 60$  km/s. In this respect we note that the Fe  $K\alpha$  line was not been detected by *XMM-Newton* during the middle of the eclipse, and the upper limit on the line flux is  $\sim 10$  or less of that measured outside the eclipse. This in turn sets an upper limit on a potential contribution to the emission of this line by a wind or some sort of circumstellar material. There is no Doppler signature of a wind in the HETG spectrum of the Fe K line (Jimenez-Garate et al. 2003), and the wind would have to be enclosed by the Roche lobe due to the absence of Fe K in eclipse.

On the other hand, taken as a body the data reported here suggest a complex origin for the overall emission of the Fe  $K\alpha$  line. To our knowledge, a complex of lines which include all ionization states from Fe XVIII to XXIV Fe  $K\alpha$  has not been observed in any astrophysical source. This may still indicate an outflow of relatively cold gas or some complex dynamics in the disk/magnetosphere interface. Such phenomena should be time-dependent and may be monitored in the future using *Astro-E2*.

#### 6.4 The $\sim 7$ keV Fe line

Our observations have revealed an Fe XXVI line at  $\sim 7$  keV, detected during low-state. The line is not detected during the main-on when the X-ray spectrum is dominated by the strong continuum emission. This feature has not been detected by Leahy et al. (2001) using *Ginga* data. However, *Ginga* has a relatively low spectral resolution around these energies (18 percent at 6 keV). *ASCA* observed the source with better spectral resolution (2 percent at 5.9 keV using the SIS detectors) during an early main on state, and based on these data Endo et al. (2000) reported the first resolution of the broad feature into two components, at 6.41 keV and 6.73 keV. However, this double structure has not been detected in other observations taken during the main-on nor is it present in *XMM-Newton* data at similar phases.

The EPIC detectors on board *XMM-Newton* have a spectral resolution similar to *ASCA* at 6 keV. However, *XMM-Newton* has a much greater effective area allowing lines to be detected with a greater confidence, in particular during the states of low intensity of the binary system. The feature at  $\sim 7$  keV has been observed by *XMM-Newton* for the first time over several 35 day phases. Also, it has been confirmed by a *Chandra* HETGS observation of the source (the only one made during the low state) taken at  $\Phi_{35} = 0.44 - 0.46$  (Jimenez-Garate et al. 2003). The feature cannot be produced by fluorescence, and it is more likely to be a Fe XXVI line originating in widely extended photo-ionized plasma. On the other hand, RGS data taken during the low and short-on states also show the presence of photo-ionized gas (Jimenez-Garate et al. 2002). Grating spectra exhibit several narrow recombination emission lines, the most prominent being C VI, N VI, N VII, O VII, O VIII and Ne IX. The line ratio  $G = (f + i)/r$ , as computed for all the helium-like ion complexes, is  $G \simeq 4$ , which indicates that photoionization is the dominant mechanism.\* Moreover, RGS spectra shows two radiative recombination continua of O VII and N VII, consistent with a low temperature of the emitting plasma ( $30000 \text{ K} < T < 60000 \text{ K}$ , Jimenez-Garate et al. 2002), which furtherly validate the photoionization model. None of these features is detected during the main-on state (where instead there might be evidence for a broad O VII i line, and perhaps O VIII Ly alpha). The recombination X-ray line emission are not likely to originate in HZ Her, due to the absence of UV induced photoexcitation signatures in the He-like triplets (observed with HETGS, Jimenez-Garate private comm.).

Instead, as suggested by Jimenez-Garate et al. (2002), an extended, photoionized accretion disk atmosphere and corona may be responsible for such features. Jimenez-Garate et al. (2001) computed the spectra of the atmospheric layers of a Shakura-Sunyaev accretion disk, illuminated by a central X-ray continuum. They found that, under these conditions, the disk develops both an extended corona which is kept hot at the Compton temperature, and a more compact, colder, X-ray recombination-emitting atmospheric layer (see Figure 9 in Jimenez-Garate et al. 2002). The parameters of the compact atmospheric layer are consis-

\* Here  $i$ ,  $r$  and  $f$  denote the intercombination line blend, the resonance line and the forbidden line; for collisionally ionized gases it is  $G < 1$  (Liedahl 1999, Porquet & Dubau 2000).

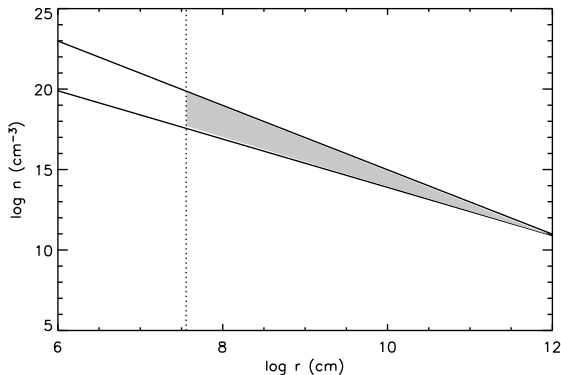


**Figure 10.** Electron density plotted versus the size of the region enclosing the Fe XXVI line emitting plasma. The three lines are the constraints discussed in the text and the shadowed region is allowed.

tent with the constraints to the narrow line emitting region, as derived from spectroscopic analysis and modeling of the RGS features.

Interestingly, the Fe XXVI line detected by *XMM-Newton* may be a signature of the *hottest* external layers of the disk corona, which are located above the recombination-emitting layers. In order to detect a line at  $\sim 7$  keV, an ionization parameter  $\log \xi \geq 3.3$  is required (Kallman and McCray 1982, their Fig. 1b). Using the flux of power law component reported by R02 (i.e.  $3.65 \times 10^{-8}$  erg/cm<sup>2</sup>/s at  $\Phi_{35} = 0.17$ ) and a source distance of 6.6 kpc, the luminosity of the direct beam is  $L_x = 1.9 \times 10^{38}$  erg/s. This gives

$$nr^2 \equiv \frac{L_x}{\xi} < 9.7 \times 10^{34} \text{ cm}^{-1}, \quad (1)$$

where  $n$  is the particle density and  $r$  is the size of the region enclosing the Fe XXVI line emitting plasma. A second constraint can be derived from the emission measure. Running a detailed multi-temperature plasma model in XSTAR gives an emission measure of  $n^2V > 6.1 \times 10^{57}$  cm<sup>-3</sup> for the 7 keV line, for a flux of  $2 \times 10^{-4}$  photons/cm<sup>2</sup>/s (the emission measure scales linearly with the line flux, and the latter varies between  $1 - 2 \times 10^{-4}$  photons/cm<sup>2</sup>, see Figure 6)<sup>†</sup>. The average temperature, computed by using a main-on custom ionization spectrum in XSTAR as well as HULLAC recombination emissivities (D. Liedahl, private comm.), is  $kT \sim 580$  eV. Moreover, if the line emitting plasma is located outside the Alfvén shell,  $r > 3.6 \times 10^7$  cm. These three constraints define an allowed region in the plane  $n-r$ , which is shown in Figure 10. The density of the hot coronal layers in the disk models by Jimenez-Garate et al. (2001) is  $10^{15} - 10^{16}$  cm<sup>-3</sup> if the radius is  $r \sim 10^8 - 10^{10}$  cm, therefore within the limits shown in the figure.

In summary, the variability of the Her X-1 spectrum lends support to the precession of the accretion disk. The evidence for the disk identification relies on the modeled

structure and spectra from a photoionized disk (Jimenez-Garate et al. 2001), which is in agreement with the limit set spectroscopically on the density of the low-energy lines emitting region. Interestingly, the same model naturally provides a candidate for the region emitting the Fe XXVI line and again the computed values of the density agree with the constraints inferred from the line parameters. Taken together, these facts strengthen the interpretation of the low state emission in term of an extended source and open the exciting possibility to monitor spectroscopically the different atmospheric components of the disk during the transition from the low to the high state.

## 7 ACKNOWLEDGMENTS

We would like to thank the referee, Arvind Parmar, for a careful reading of the manuscript. Based on observations obtained with XMM-Newton, an ESA science mission with instruments and contributions directly funded by ESA Member States and the USA (NASA). This paper makes use of quick-look results provided by the ASM/RXTE team whom we thank.

## REFERENCES

- Asai, K., Dotani, T., Nagase, F., & Mitsuda, K., 2000, *ApJS*, 131, 571
- Baykal, A., Boynton, P. E., Deeter, J. E., & Scott, D. M., 1993, *MNRAS*, 267, 347
- Boroson, B., Kallman, T., & Vrtilik, S.D., 2001, *ApJ*, 562, 925
- Cash, W., 1979, *ApJ*, 228, 939
- Choi, C.S., Nagase, F., Makino, F., Dotani, T., Kitamoto, S., & Takahama, S. 1994, *ApJ*, 437, 449
- Coburn, W., Heindl, W. A., Wilms, J., Gruber, D. E., Staubert, R., Rothschild, R. E., Postnov, K. A., Shakura, N., Risse, P., Kreykenbohm, I., & Pelling, M. R., 2000, *ApJ*, 543, 351
- Deeter, J.E., Scott, D. M., Boynton, P. E., Miyamoto, S., Kitamoto, S., Takahama, S., & Nagasem F. 1998, *ApJ*, 502, 802
- Dhillon, V. S., Marsh, T. R., & Jones, D. H. P., 1997, *MNRAS*, 291, 694
- Dotani, T., Kii, T., Nagase, F., Makishima, K., Ohashi, T., Sakao, T., Koyama, K., & Tuohy, I., 1989, *PASJ* 41, 427
- Drew, J., 1997, in *IAU colloquium 197, Accretion Phenomena and Related Outflows*, ed. D.T. Wickramasinghe, L. Ferrario, & G.V. Bicknell (ASP Conf. Ser., 121; San Francisco:ASP), 465
- Endo, T., Nagase, F., & Mihara, T. 2000, *PASJ*, 52, 223
- Groot, P. J., Rutten, R. G. M., & van Paradijs, J., 2000, *NewAR*, 44, 137
- Gerend, D., & Boynton, P., 1976, *Apj*, 209, 562
- Heemskerck, M. H. M., & van Paradijs, J., 1989, *A&A*, 223, 154
- Jimenez-Garate, M. A., Raymond, J. C., Liedahl, D. A., & Hailey, C. J., 2001, *ApJ*, 558, 448
- Hailey, C. J., den Herder, Jimenez-Garate, M. A., Hailey, C. J., den Herder, J.-W., Zane, S., & Ramsay, G., 2002, *ApJ*, 578, 391
- Jimenez-Garate, M.A., Raymond, J. C., Liedahl, D. A., & Hailey, C.J., 2003, *ApJ* submitted
- Kallman, T.R., & McCray, R., 1982, *ApJS*, 50, 263
- Kallman, T.R., Angelini, L., Boroson, B., & Cottam, J., 2003, *ApJ*, 583, 861
- Lamb, F.K., Pethick, C.J., & Pines, D., 1973, *ApJ*, 184, 271
- Leahy, D.A., 2001, *ApJ*, 547, 449
- Levine, A., Rappaport, S., Putney, A., Corbet, R., & Nagase, F., 1991, *ApJ*, 381, 101

<sup>†</sup> The value of the emission measure is consistent with calculations by Kallman et al. (2003), who found  $10^{57}$  cm<sup>-3</sup> for an accretion disk corona at 7 kpc and a Fe XXVI line with a roughly similar flux level.

- Liedahl, D.A., Wojdowski, P., Jimenez-Garate, M.A., & Sako, M., 2001, in ASP Conf. Ser. 247, Spectroscopic Challenges of Photoionized Plasmas, ed. G. Ferland & D. W. Savin (San Francisco: ASP), 447
- Mason, K. O., Breeveld, A., Much, R., Carter, M., Cordova, F. A., Cropper, M. S., Fordham, J., Huckle, H., Ho, C., Kawakami, H., and 9 coauthors, 2001, *A&A*, 365, L36
- Mavromatakis, F., 1993, *A&A*, 273, 147
- McCray, R.A., Shull, J. M., Boynton, P. E., Deeter, J. E., Holt, S. S., & White, N. E. 1982, *ApJ*, 262, 301
- Mihara, T., Ohashi, T., Makishima, K., Nagase, F., Kitamoto, S., & Koyama, K., 1991, *PASJ*, 43, 501
- Ogelmen, H., & Trümper, J., 1988, *MmSAI*, 59, 169
- Oosterbroek, T., Parmar, A. N., Martin, D. D. E., & Lammers, U., 1997, *A&A*, 327, 215
- Oosterbroek, T., Parmar, A. N., Dal Fiume, D., Orlandini, M., Santangelo, A., Del Sordo, S., & Segreto, A., 2000, *A&A*, 353, 575
- Oosterbroek, T., Parmar, A. N., Orlandini, M., Segreto, A., Santangelo, A., & Del Sordo, S., 2001, *A&A*, 375, 922
- Parmar, A. N., White, N.E., & Stella, L., 1989, *ApJ*, 338, 373
- Parmar, A. N., Oosterbroek, T., dal Fiume, D., Orlandini, M., Santangelo, A., Segreto, A., & del Sordo, S., 1999, *A&A*, 350, L5
- Palmeri, P., Mendoza, C., Kallman, T. R. & Bautista, M. A., 2003, *A&A*, 403, 1175
- Porquet, D. & Dubau, J., 2000, *A&AS*, 143, 495
- Ramsay G., Zane S., Jimenez-Garate M. A., den Herder J.-W., & Hailey C. J., 2002, *MNRAS*, 337, 1185 (R02)
- Scott, M. D., Leahy, D. A., & Wilson, R. B., 2000, *ApJ*, 539, 392
- Still M., O'Brien K., Horne K., Hudson D., Boroson B., Vrtiliek S. D., Quaintrell H., & Fiedler H., 2001, *ApJ*, 553, 776
- Strüder, L., Briel, U., Dennerl, K., Hartmann, R., Kendziorra, E., Meidinger, N., Pfeffermann, E., Reppin, C., Aschenbach, B., Bornemann, W., and 48 coauthors, 2001, *A&A*, 365, L18
- Sunyaev, R. A., Gilfanov, M. R., Churazov, E. M., Loznikov, V. M., Efremov, V. V., Kaniovskii, A. S., Kuznetsov, A. V., Melioranskii, A. S., Voges, W., Pietsch, W., and 11 coauthors, 1988, *SvAL*, 14, 416
- Turner, M. J. L., Abbey, A., Arnaud, M., Balasini, M., Barbera, M., Belsole, E., Bennie, P. J., Bernard, J. P., Bignami, G. F., Boer, M., and 53 coauthors, 2001, *A&A*, 365, L27
- Watanabe, S., Sako, M., Ishida, M., Ishisaki, Y., Kahn, S.M., Kohmura, T., Morita, U., Nagase, F., Paerels, F., & Takahashi, T., 2003, *ApJ*, 597, L37
- Vrtiliek, S. D., & Cheng, F.H., 1996, *ApJ*, 465, 915